

## Effect of sidewall conductance on heat-transport measurements for turbulent Rayleigh-Bénard convection

Guenter Ahlers

*Department of Physics and iQUEST, University of California, Santa Barbara, California 93106*

(Received 31 July 2000; published 27 December 2000)

For measurements of turbulent heat transport in Rayleigh-Bénard convection the correction for the sidewall conductance is usually neglected or based on measurements or estimates for the empty cell. It is argued that the lateral thermal coupling between the fluid and the wall can invalidate these approaches, and that corrections based on calculations of the two-dimensional temperature fields are required in some cases. These corrections can increase  $\gamma$  obtained from fits of  $\mathcal{N}=\mathcal{N}_0R^\gamma$  ( $R$  is the Rayleigh number) to the Nusselt number  $\mathcal{N}(R)$  by 0.02 or more, yielding values in the range 0.30 to 0.33, which are larger than most theoretical predictions.

DOI: 10.1103/PhysRevE.63.015303

PACS number(s): 47.27.-i, 44.25.+f, 47.27.Te

One of the important issues in turbulent convection of a fluid heated from below is the global heat transport of the system [1], as expressed by the Nusselt number

$$\mathcal{N}=\lambda_{eff}/\lambda; \quad \lambda_{eff}=qL/\Delta T. \quad (1)$$

Here  $q$  is the heat-current density,  $L$  the sample height,  $\Delta T=T_h-T_c$  the temperature difference, and  $\lambda$  the conductivity of the quiescent fluid. Usually a powerlaw

$$\mathcal{N}=\mathcal{N}_0R^\gamma \quad (2)$$

is fitted to the data. Here  $R\equiv\alpha gL^3\Delta T/\kappa\nu$  is the Rayleigh number, with  $\alpha$  the isobaric thermal expansion coefficient,  $g$  the gravitational acceleration,  $\kappa$  the thermal diffusivity, and  $\nu$  the kinematic viscosity. Various data sets for Prandtl numbers  $\sigma\equiv\nu/\kappa\geq 0.66$  yielded values of  $\gamma$  from 0.28 to 0.31 [1,2]. Several theoretical models made predictions of  $\gamma$  in a similar range [1].

To determine  $\mathcal{N}$  from Eq. (1), the heat current applied to the cell bottom must be corrected for the part passing through the sidewall. In all cases I know of this correction is based on measurements or estimates for the empty cell or assumed to be negligible. Unfortunately, in several cases neither is a good approximation. The reason is that the vertical temperature variation in the fluid is mostly across boundary layers (BLs) near the top and bottom, with a nearly uniform temperature over most of the cell interior. The thermal coupling of the temperature profile of the wall to that of the fluid then yields relatively large temperature gradients in the wall near the ends. Consequently the current entering (leaving) the wall at the cell bottom (top) usually is much larger than for an empty cell. Although this may seem obvious, its neglect significantly reduced the results for  $\gamma$  in several experiments. Corrections based on numerical calculations of the two-dimensional temperature field in the cell and wall increase  $\gamma$  by 0.02 or more for some experimental wall-fluid combinations, yielding values well above most theoretical predictions [1].

For a more quantitative examination, let the vertical  $z$  axis be pointing downward with its origin at the cell center, and define  $H\equiv L/2$ . Let a fixed current  $Q=Q_F+Q_W$  be applied at  $z=H$ , with  $Q_F$  and  $Q_W$  flowing through the fluid and sidewall respectively. Numerical calculations [3] of the tem-

perature field based on simplified models of the turbulent system were carried out for several sidewall-fluid combinations with sidewalls of uniform width  $d_w$ , which terminated abruptly at the top and bottom plates. These plates were assumed to provide constant-temperature boundary conditions  $T_h=1$  and  $T_c=-1$  below and above the system respectively. The fluid was represented by three quiescent BLs of conductivity  $\lambda$  and an interior of uniform temperature  $T_0=(T_h+T_c)/2$ . Two BLs were of thickness  $l=L/2\mathcal{N}$  and located near  $z=\pm H$  parallel to the top and bottom plates [4]. The third was parallel to the sidewall, but its nature is more ambiguous. One model (Mod. 1) assumes a laminar viscous BL [5] and assigns to it a fixed average thickness [2]  $l_v=0.25LR_e^{-1/2}$  which is determined by the Reynolds number [2]  $R_e=0.039R^{1/2}\sigma^{-5/6}$  ( $R_e=0.037R^{1/2}\sigma^{-3/4}$ ) of a large-scale flow for  $\sigma\geq 2$  ( $\sigma\approx 0.7$ ). Although this is in good agreement with measurements of the time-averaged velocity for  $\sigma=7$  [6], the velocity in the BL fluctuates [6]. Presumably the fluctuations enhance the effective thermal conductivity. Thus, assigning the fluid conductivity  $\lambda$  to this BL probably overestimates the thermal barrier provided by it between the turbulent interior and the wall. Another problem may be that for large  $L$  and modest  $R$  the model predicts values of  $l_v$  in excess of 1 cm. It seems unlikely that such a thick vertical layer will be stable in the presence of the vigorously turbulent flow adjacent to it, and in the presence of gravity. Thus, as an alternative, a thin BL of fixed  $l_v=0.1$  cm with conductivity  $\lambda$  was used as a second model (Mod. 2). This one probably underestimates the thermal barrier, with the physical case somewhere between the two models. The lateral coupling between the wall and the fluid assures that  $Q_w(z)$  [and thus also  $Q_f(z)$ ] depends on  $z$ . It was assumed that the relevant correction is  $Q_w(-H)=Q_w(H)$  at the ends where the horizontal BLs in the fluid are located, although this may be an issue deserving further consideration. The cylindrical sample was approximated by a two-dimensional thin-slab model which may be viewed as a sheet of unit width and uniform temperature in the  $y$  direction, with a length in the  $x$  direction equal to  $d_w(1+A/A_w)$  ( $A_w$  and  $A$  are the cross sectional areas of the wall and the fluid), and a height  $L$  in the  $z$  direction. This preserves the ratio of the cross sectional areas of the wall and the fluid, and should be a good approximation when the cell diameter is much larger

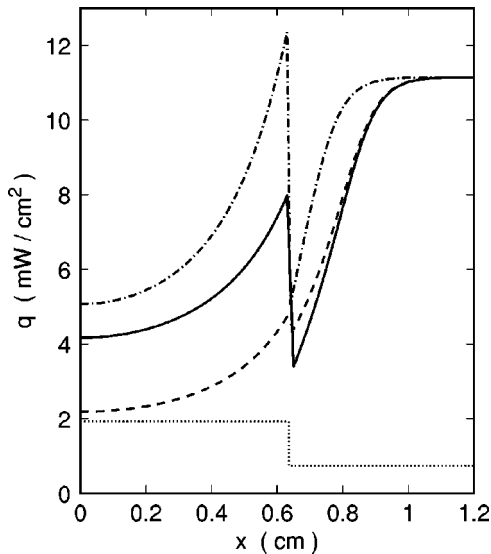


FIG. 1. Heat-current density  $q(x, H)$  entering the wall and fluid at the bottom ( $z=H$ ) for  $\mathcal{N}=15$ . Solid line, HDPE wall and Mod. 1 [case 2, Table I, same as Fig. 2(a)]. Dashed line, Plexiglas wall and Mod. 1 (case 1, Table I). Dash-dotted line, HDPE wall (case 2, Table I) and Mod. 2. The dotted line gives the current that would prevail for HDPE if the gradient in the system were vertical and equal to  $\Delta T/L$ .

than the wall thickness. Only the lower half  $0 \leq z \leq H$  was simulated, since the problem is symmetric about the horizontal midplane. Only a horizontal section  $0 \leq x \leq (d_w + l_v + 4l)$  was solved numerically. The contribution from  $x > (d_w + l_v + 4l)$  was represented by a constant temperature gradient in the BL and  $T=T_0$  above it. The current density  $q(x, z=H) = \lambda(x)(dT/dz)_{z=H}$  with  $\lambda(x)$  the conductivity of the material at lateral position  $x$  (either wall or fluid) was computed. Examples are shown in Fig. 1. The sums of  $q(x, H)$ , separately over the wall and fluid domain of  $x$ , gave  $Q_W(H)$  and  $Q_F(H)$ . The fractions

$$f_W = Q_W(H)/Q, \quad f_F = 1 - f_W \quad (3)$$

were then calculated. The corrected  $\mathcal{N}$  is given by  $\mathcal{N} = f_F \tilde{\mathcal{N}}$  if the wall current was originally neglected, i.e., if  $\tilde{\mathcal{N}} = QL/A\Delta T\lambda$  [7].

Examples of the calculated temperature fields for  $\mathcal{N} = 15$  ( $R \approx 5 \times 10^6$ ) and 50 ( $R \approx 4 \times 10^8$ ) for case 2 of Table I

TABLE I. Parameters for examples of  $f_F$ . The walls are Plexiglas (PI), HDPE (PE), stainless steel (SS).

Case	Fluid	$\lambda$ W/m K	Wall	$\lambda_w$ W/m K	$d_w$ cm	$L$ cm	$\Gamma$	Ref.
1	ethanol	0.167	PI	0.19	0.635	4.5	2.0	
2	ethanol	0.167	PE	0.43	0.635	4.5	2.0	
3	He gas	0.011	SS	0.24	0.05	20	0.5	[8]
4	He gas	0.011	SS	0.24	0.27	100	0.5	[9]
5	He gas	0.011	SS	0.24	0.15	40	0.5	[10]
6	water	0.616	PI	0.19	0.16	10	0.5	

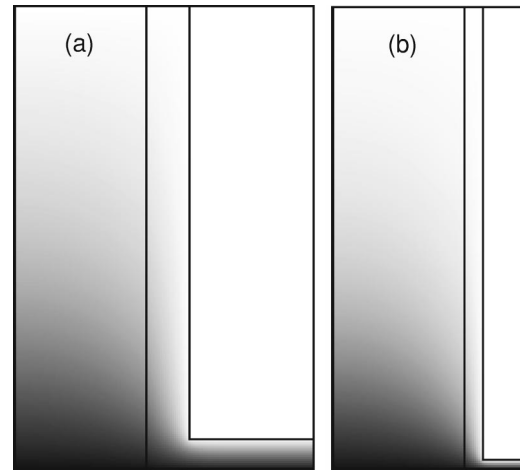


FIG. 2. Temperature fields for case 2 of Table I and Mod. 1. White,  $T_0$ ; black,  $T_h$ . (a)  $\mathcal{N}=15$ ; (b),  $\mathcal{N}=50$ . Only the lower half of the portion near the sidewall is shown.

and Mod. 1 are presented in Fig. 2. The vertical line extending throughout the entire system is the fluid-wall boundary. To the left and below the “L”-shaped line the fluid is assumed to be quiescent, with a conductivity  $\lambda$ . Above and to the right of it  $T=T_0$ . One sees that the temperature variation in the wall is largest near the cell bottom, leading to an enhanced wall current near  $z=H$ . This is seen more clearly in Fig. 1, which gives  $q(x, H)$  for the example in Fig. 2(a) ( $\mathcal{N}=15$ ) with a high-density polyethylene (HDPE) sidewall (solid and dash-dotted lines), and for the same geometry with a Plexiglas sidewall (dashed line). The dotted line is the current that would prevail for HDPE if the entire system had a uniform vertical temperature gradient equal to  $\Delta T/L$ . Near the right-hand side of the figure the convection enhances the heat transport by a factor  $\mathcal{N}=15$  regardless of the wall. In the range  $0.635 < x \leq 0.9$  the effect of the viscous boundary layer of width 0.21 cm (solid line, Mod. 1) or 0.1 cm (dash-dotted line, Mod. 2) is noticed. At  $x=0.635$  the temperature gradient at  $z=H$  is continuous but, because of the discontinuity of the conductivity, the current density  $q(x, H)$  is discontinuous. In the wall ( $x < 0.635$ ) the current decreases as  $x$  decreases, but because of the adiabatic boundary condition at the outside of the wall the horizontal gradient has to vanish there. For Mod. 1, integration of  $q(x, H)$  for these examples yields  $f_F = 0.869$  (0.924) for HDPE (Plexiglas). For comparison, the (inappropriate) constant-temperature-gradient approximation would yield 0.970 (0.982) for HDPE (Plexiglas).

To demonstrate the relevance of  $f_F$ , Fig. 3 shows new measurements corresponding to cases 1 and 2 in Table I in the form of  $\log_{10}(\mathcal{N}R^{-2.7})$  versus  $\log_{10}(R)$ . The closed (open) symbols are for a HDPE (Plexiglas) sidewall. For the circles the sidewall correction was neglected. The two data sets differ from each other by about 5%. The squares were obtained after multiplying by  $f_F$  based on Mod. 1. The agreement is very good. The diamonds result when Mod. 2 is used. The agreement now is perfect for  $R \leq 7 \times 10^7$ . The small deviations of 1.5% or less for larger  $R$  are not understood, but may be associated with inadequacies of the model

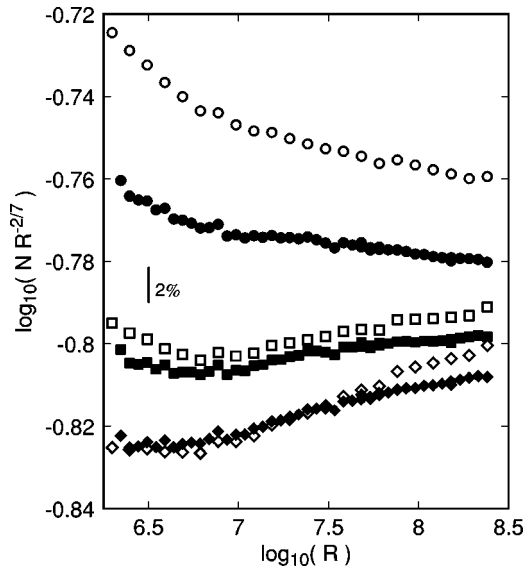


FIG. 3. Measurements of  $\mathcal{N}$  for cases 1 and 2 in Table I. Open (closed) symbols are for a HDPE (Plexiglas) wall. Circles, without sidewall correction; squares, with correction using Mod. 1; diamonds, with correction using Mod. 2 (the data were shifted downward by 0.01).

when the horizontal BLs become very thin. The change in  $\gamma$  at  $R=3 \times 10^7$  is 0.018 (0.012) for Mod. 1 and 0.030 (0.017) for Mod. 2 for the HDPE (Plexiglas) wall.

The above analysis suggests that the nature of the wall near the top and bottom plates matters much more than the central section. Unfortunately, complicated and often unpublished sidewall geometries involving flanges and seals, as well as the approximations in the treatment of the vertical BL, prevent a quantitative calculation of the correction appropriate for published values of  $\mathcal{N}$ . Nonetheless it is possible to get a rough idea about the effect of  $f_F$  on the data. Thus,  $f_F(\mathcal{N})$  for the cases listed in Table I and Mod. 1 is shown in Fig. 4 as solid lines. Cases 3, 4, and 5 correspond approximately to the experiments of the references in the last column of the table. One sees that the correction is relatively large for the gaseous helium experiments. This is so because the conductivity ratio  $\lambda_w/\lambda$  is relatively large. But even for them  $f_F$  is close to one and the wall correction less than a few percent for  $\mathcal{N} \geq 10^3$  ( $R \geq 5 \times 10^{12}$ ). At the other extreme, an exceptionally thin low-conductivity Plexiglas wall and a relatively high-conductivity fluid (water) yield a nearly negligible correction for all  $\mathcal{N}$  (case 6). Figure 4 also illustrates the dependence of  $f_F$  on  $l_v$ . The broken lines are for Mod. 2 for cases 1 to 5 (see the caption).

In order to get an estimate of the impact which the wall correction has on published data, the original as well as the corrected [7] results from Refs. [8–10] are shown in Fig. 5. A fit over the range  $10^8 \leq R \leq 10^{12}$  of Eq. (2) yields  $\gamma = 0.314, 0.306,$  and  $0.289$  for the original data,  $0.327, 0.320,$  and  $0.304$  for the corrected data using Mod. 1, and  $0.334, 0.334,$  and  $0.317$  for the corrected data using Mod. 2 for Refs. [8–10] respectively. The corrected values are larger than the pure powerlaw exponents predicted by various theoretical models [1]. Of course a more quantitative evalua-

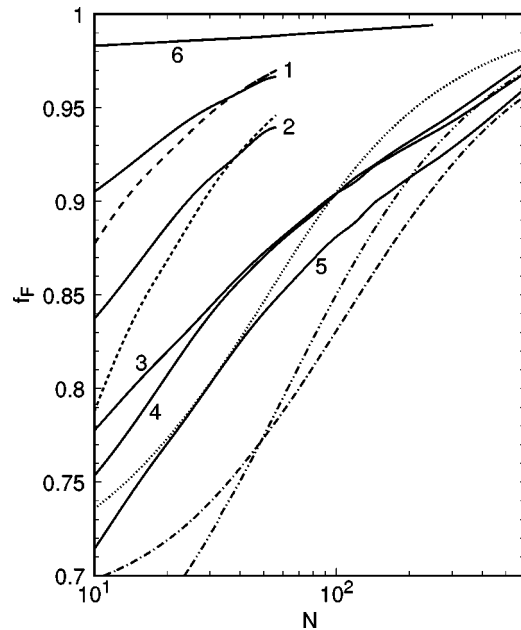


FIG. 4. Fraction  $f_F$  of  $Q$  entering the fluid at  $z=H$  for cases listed in Table I. The solid lines, labeled by the cases of Table I, are for Mod. 1. The broken lines are for Mod. 2 and correspond to case 1 (long dashed line), 2 (short dashed line), 3 (dotted line), 4 (dash-dotted line), and 5 (dash-double-dotted line).

tion, which can only be carried out with consideration of the precise experimental sidewall geometry and a more quantitative treatment of the BL along the wall, would be desirable.

Figure 6 shows the recent data of Xu *et al.* [11] obtained with acetone and HDPE walls [12]. Here also the Nusselt

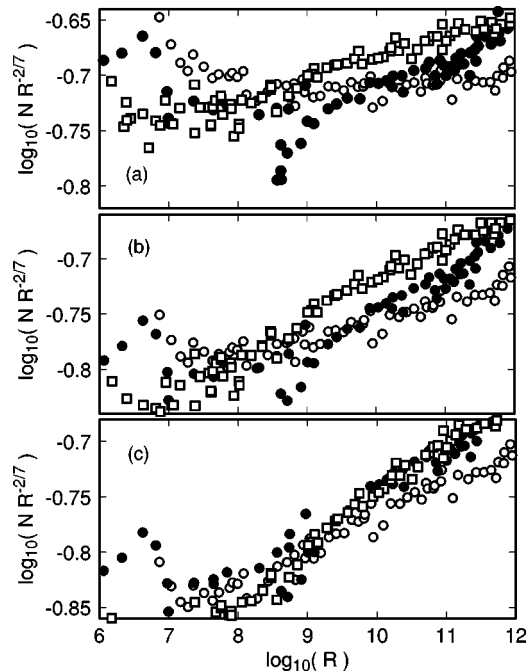


FIG. 5. Measurements of  $\mathcal{N}(R)$  by Chavanne *et al.* ([8], closed circles), Niemela *et al.* ([9], open squares), and Wu ([10], open circles). (a), original data; (b), after wall correction using Mod. 1; (c), after wall correction using Mod. 2.

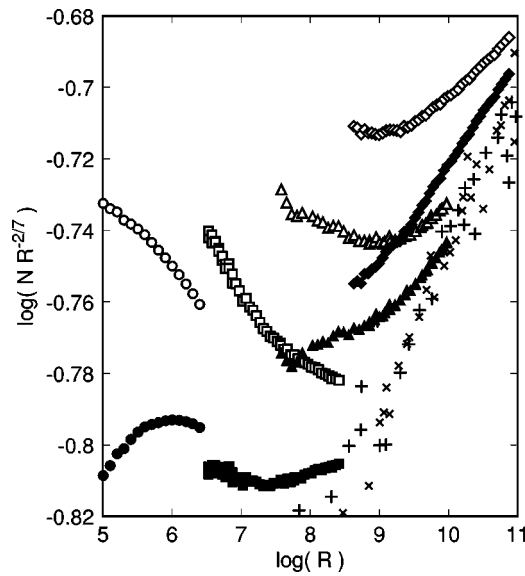


FIG. 6. Nusselt-number measurements from Ref. [11] as a function of the Rayleigh number on logarithmic scales. Open symbols, original data [12]; solid symbols, corrected data; circles, aspect ratio  $\Gamma=12.8$ ; squares,  $\Gamma=3.0$ ; triangles,  $\Gamma=1.0$ ; diamonds,  $\Gamma=0.5$ ; plusses, corrected data of Ref. [8]; crosses, corrected data of Ref. [9]. In this figure all corrected data are based on Mod. 1.

number is reduced by the wall effect and the effective exponents are increased. For  $R=10^7$ ,  $10^9$ , and  $10^{10}$ , for instance, the  $\Gamma=3$ , 1.0, and 0.5 data give  $\gamma=0.253$  (0.272 and 0.280), 0.282 (0.288 and 0.295), and 0.301 (0.308 and 0.314) respectively when the wall conductance is ignored (included with Mod. 1 and with Mod. 2). For comparison, the corrected data of Refs. [8] and [9] for  $\Gamma=0.5$  using Mod. 1 are shown as well (those of Ref. [10] were omitted to avoid overcrowding).

One of the main conclusions of Ref. [11] was that data for  $\mathcal{N}(R)$  cannot be fit by a single powerlaw over a wide range of  $R$ , but that nonetheless there exists a scaling function  $F(R)=\mathcal{N}(R,\Gamma)/f(\Gamma)$  with  $f(\Gamma)=\mathcal{O}(1)$ . Within their uncer-

tainty the corrected data are also consistent with these conclusions. However, for  $7.3 \leq \log(R) \leq 9.3$  they can also be interpreted to imply that a powerlaw with  $\gamma=0.289$  (0.292) is applicable when Mod. 1 (Mod. 2) is used. The data are then consistent with a transition at  $\log(R) \approx 9.3$  to a regime with  $\gamma=0.309$  (0.316) for Mod. 1 (Mod. 2) which was obscured in the original data by rounding due to the wall contribution. This issue will require more careful study in the future. Another conclusion [11] was that the Grossmann-Lohse prediction [2]  $\mathcal{N}=a\sigma^{-1/12}R^{1/4}+b\sigma^{-1/7}R^{3/7}$  fits the data. This is still true for the corrected data within their possible systematic errors, albeit only for  $R \geq 10^8$ . The new coefficients  $a=0.312$  (0.298) and  $b=0.00256$  (0.00291) for Mod. 1 (Mod. 2) differ slightly from the original estimates [11]  $a=0.326$  and  $b=0.00236$ .

In this Rapid Communication it was argued that the lateral thermal coupling between the fluid and the wall in turbulent Rayleigh-Bénard convection can require that the correction for the current passing through the wall be based on a two-dimensional calculation of the temperature field of the system. Simply subtracting the conductance of the empty cell can lead to errors of 20% or more of the Nusselt number  $\mathcal{N}$  in unfavorable cases, and can yield a systematic underestimate by 0.02 or more of the exponent  $\gamma$  obtained from a power-law fit to the data. The wall correction can be significant for Rayleigh numbers up to  $10^{12}$  or so. This work also suggests improvements in the design of future convection cells which will minimize the wall current. Obviously the sidewalls must be made as thin as possible and constructed of the lowest-conductivity material consistent with the fluid to be used. Equally important, the sidewall should extend parallel to the sides of the top and bottom plates with any flanges, seals, or gaskets located well away from the active surface of these plates.

I benefitted from stimulating conversations with J. Niemela and K.R. Sreenivasan. This work was supported by the National Science Foundation through Grant No. DMR00-71328.

- [1] For a reviews, see, for instance, E.D. Siggia, *Annu. Rev. Fluid Mech.* **26**, 137 (1994).  
 [2] S. Grossmann and D. Lohse, *J. Fluid Mech.* **407**, 27 (2000).  
 [3] H. Schenk, Jr., *Fortran Methods in Heat Flow* (The Ronald Press Co., New York, 1963); M. Necati Ozisik, *Boundary Value Problems of Heat Conduction* (International Textbook, Scranton, PA, 1968).  
 [4] A. Belmonte, A. Tilgner, and A. Libchaber, *Phys. Rev. Lett.* **70**, 4067 (1993); *Phys. Rev. E* **50**, 269 (1994); A. Tilgner, A. Belmonte, and A. Libchaber, *Phys. Rev. E* **47**, R2253 (1993).  
 [5] L.D. Landau and E.M. Lifshitz, *Fluid Mechanics* (Pergamon, London, 1959), Chap. IV.  
 [6] X.-L. Qiu and K.-Q. Xia, *Phys. Rev. E* **58**, 486 (1998).  
 [7] In cases where the correction was applied to published data [8–10] which had originally been obtained by subtracting the conductance of the empty cell from  $Q$ , the correction factor

$f_F(\mathcal{N})/[1-f_W(1)/\mathcal{N}]$  was applied.

- [8] X. Chavanne, F. Chilla, B. Chabaud, B. Castaing, J. Chaussy, and B. Hébral, *J. Low Temp. Phys.* **104**, 109 (1996).  
 [9] J.J. Niemela, L. Skrbek, K.R. Sreenivasan, and R.J. Donnelly, *Nature (London)* **404**, 837 (2000).  
 [10] X.Z. Wu, Ph.D. thesis, University of Chicago, 1991 (unpublished). The data were re-evaluated on the basis of new fluid properties by Niemela *et al.* (private communication).  
 [11] X. Xu, K.M.S. Bajaj, and G. Ahlers, *Phys. Rev. Lett.* **84**, 4357 (2000).  
 [12] The original data [11] were re-evaluated using new measurements of the relevant fluid properties, and with a more accurate experimental determination of the series resistance due to a boundary layer in the water bath immediately above the sapphire top plate of the cell. For the open symbols in Fig. 6 no wall correction was applied.